

# Thermal Evolution and Structural Study of Cobalt Doped Magnesium Aluminate Spinel Nanoparticles Prepared by Coprecipitation Technique

Dr. Shyam Sunder\* and Dr. Wazir Singh

Department of Applied Science & Humanities, Ch. Devi Lal State Institute of Engineering & Technology  
Panniwala Mota, Sirsa, India

\*Corresponding author: shyampph@yahoo.com

## ABSTRACT

Introduction of transition metal (  $M = \text{Co, Fe, Ni, V, Cr, Mn, Ca, Ba, Sr}$  ) in  $\text{MgAl}_2\text{O}_4$  spinel have attracted a lot of interest of researchers as well as technologists due to its excellent absorption, emission and luminescence properties potential use. Among various transition metals,  $\text{Co:MgAl}_2\text{O}_4$  can be regarded as a good candidate for such applications to the high mechanical resistance, high thermal and chemical stability, and low temperature sinterability of spinel type oxide materials. The physical properties of  $\text{Co:MgAl}_2\text{O}_4$  like chemical strength, catalytic ability, and high temperature resistivity have been further enhanced. Cobalt-magnesium aluminate crystallizes at relatively higher temperature, i.e. above  $850^\circ\text{C}$  as compared to undoped magnesium aluminate that crystallizes around  $800^\circ\text{C}$ . A single phase  $\text{Co:MgAl}_2\text{O}_4$  face centred cubic ordered-spinel nanopowder (grain size  $\sim 20$  nm) with a good, chemical homogeneity, is obtained by using co-precipitation method followed by thermal treatment at temperature  $1000^\circ\text{C}$  for 4h, in air.

**Keywords :** Magnesium Aluminate, Cobalt, Nanoparticle, Coprecipitation, Structure Characterization.

## I. INTRODUCTION

The effects of heat treatment on structural evolution, lattice constant micro-strain and grain size of magnesium aluminate spinel powders prepared by coprecipitation have been discussed. Introduction of transition metal ( $M = \text{Co, Fe, Ni, V, Cr, Mn, Ca, Ba, Sr}$ ) in  $\text{MgAl}_2\text{O}_4$  spinel have attracted a lot of interest of researchers as well as technologists due to its excellent absorption, emission and luminescence properties [1-6]. The traditional source of blue colour in inorganic pigments depends on cobalt ion [7]. A cobalt doped  $\text{Co}_x\text{Mg}_{1-x}\text{Al}_2\text{O}_4$  ( $0 < x < 1$ ) has been used in reduction of the production costs and environmental problems [8]. Moreover owing to the high mechanical resistance, high thermal and chemical stability, and low temperature sinterability

of spinel type oxide materials,  $\text{Co}_x\text{Mg}_{1-x}\text{Al}_2\text{O}_4$  is in great demand for qualified nano inorganic blue pigment [9]. Inorganic blue pigments are widely used in industry to bring colour to plastics, paints, fibers, papers, rubbers, glass, cement, glazes, ceramics, and porcelain enamels [10]. Among various transition metals,  $\text{Co:MgAl}_2\text{O}_4$  can be regarded as a good candidate for such applications.

Studies concerning the effect of  $\text{Co:MgAl}_2\text{O}_4$  have been carried out by several workers. Luan et. al. [11] prepared  $\text{Co}^{2+}:\text{MgAl}_2\text{O}_4$  nanocrystalline powders at low temperature  $710^\circ\text{C}$  by the solgel method much lower than the conventional solid phase reaction method. Using coprecipitation method and ammonium hydrogen carbonate as precipitating agent, pure and highly dispersed nanoscale powders

of Co-doped  $\text{MgAl}_2\text{O}_4$  were synthesized by coprecipitation method at  $800^\circ\text{C}$  with particle size in the range of 10-30 nm [12]. Iqbal et. al. [13] prepared cobalt doped  $\text{MgAl}_2\text{O}_4$  by using coprecipitation method, urea as precipitating agent and studied their physical properties of the product. These workers [14], also synthesized  $\text{Mg}_{1-2x}\text{Co}_x\text{Al}_2\text{O}_4$  nanocrystallites with large surface area by the urea combustion method in the microwave oven. Javed et. al. [15] prepared cobalt doped nanocrystalline  $\text{MgAl}_{2-x}\text{Co}_x\text{O}_4$  (where  $x = 0, 0.5, 1.0, 1.5, 2.0$ ) spinels by chemical coprecipitation method by substituting  $\text{Al}^{3+}$  ions by  $\text{Co}^{2+}$  ions thereby yielding an electron rich terminal compound with particle size 7-19 nm. Nanocrystalline  $\text{Co}_x\text{Mg}_{1-x}\text{Al}_2\text{O}_4$  spinel pigment has been synthesized via low-temperature combustion route by employing  $\beta$ -alanine as a novel environmentally benign fuel by Torkian et. al. [16]. In nanoscale, the physical properties of  $\text{Co}:\text{MgAl}_2\text{O}_4$ ; like chemical strength, catalytic ability, and high temperature resistivity have been further enhanced [15]. This is due to the fact that nanocrystalline materials have, high surface to volume ratio of the grains, have quantum confinement of charge carriers, enhanced contribution towards the electrical properties from grains and grain boundary regions, creation of holes and defects in grains, and possibility of band structure modification [17].

Authors have reported in the previous studies that the mixed metal oxide spinel  $\text{MgAl}_2\text{O}_4$  belongs to cubic space group  $\text{Fd}\bar{3}\text{m}$ . A unit cell comprises 8 tetrahedrons and 16 octahedrons. The  $\text{Mg}^{2+}$  ions are located at the centre of the tetrahedron and coordinated by  $\text{O}^{2-}$  ions with full  $\text{T}_d$  symmetry (A site) while the  $\text{Al}^{3+}$  ions are located at the centre of the octahedron coordinated by  $\text{O}^{2-}$  ions with  $\text{T}_{3d}$  symmetry (B site). The doped metal ions can substitute either A site or B site or both depending upon its valency and site type [18-22]. The location of the substituted ions is crucial in determining the overall properties of the doped  $\text{MgAl}_2\text{O}_4$ . In recent

years, a variety of techniques, such as coprecipitation [23], solid state reaction [24], hydrothermal synthesis [25], sol-gel [1] and combustion syntheses [26], have been successfully developed for the preparation of pure spinel powders. The synthesis route is very important for determining the final properties of inorganic pigment such as color, particle size, and chemical & thermal stability. The liquid combustion method has the advantage of preparing crystalline powders with nano size and high purity at low temperatures [27]. Single crystal of  $\text{MgAl}_2\text{O}_4$  doped with tetrahedral  $\text{Co}^{2+}$  ions is attractive for laser modulation [28], however, the homogeneous and bulk crystals can hardly be obtained because of the high growth temperature and all kinds of defects embedded in the crystals.

In the present work, we report synthesis of nanocrystalline  $\text{Co}_x\text{Mg}_{1-x}\text{Al}_2\text{O}_4$  spinel pigment via coprecipitation technique followed by heat treatment and characterized by applying different complementary techniques. Doped with some active ions, the spinel behaves as multifunctional material, especially doped with  $\text{Co}^{2+}$  which can offer a wide choice of solid-state saturable absorbers such as opaque ceramics of  $\text{Co}^{2+}:\text{MgAl}_2\text{O}_4$  and  $\text{Co}^{2+}:\text{ZnAl}_2\text{O}_4$  [29]. In this work, Co (2.88 wt%) has been introduced in  $\text{MgAl}_2\text{O}_4$  spinels by chemical coprecipitation technique followed by thermal treatment.

## II. EXPERIMENTAL

The coprecipitation method was used to synthesize cobalt-magnesium aluminate spinel nanopowders. The high purity reagents  $\text{Mg}(\text{NO}_3)_2 \cdot 6\text{H}_2\text{O}$  (99.99% purity Sigma Aldrich ACS grade),  $\text{Al}(\text{NO}_3)_3 \cdot 9\text{H}_2\text{O}$  (99.99% purity Sigma Aldrich ACS grade),  $\text{Co}(\text{NO}_3)_2 \cdot 6\text{H}_2\text{O}$  (99.99% purity Sigma Aldrich ACS grade) and ammonia solution (28%, Sigma Aldrich, ACS grade) were used to prepare cobalt magnesium aluminate cubic spinel nanopowders. A solution of

0.2 M nitrates was prepared in double distilled water, with Co:Mg:Al (molar ratio) = 0.1:0.9:2.0. The solutions of nitrates were mixed together for homogenization. The precursor was prepared by slowly adding the mixed salt solution into the ammonia solution under rigorous stirring, pH was maintained around 8-9 and reaction temperature was maintained at 60°C. The precursor was washed with an excess of double distilled water, many times. The washed precipitates of precursor were dried for 24 hrs at 100°C in an oven in the presence of air. The solid so-obtained was grinded in agate mortar pestle to obtain fine powder. Furthermore, powdered samples were calcined at different temperatures 550°C, 700°C, 850°C and 1000°C for 4 hours in presence of air, with heating rate 10°C min<sup>-1</sup>.

TGA-DTG-DTA was carried out by model SII 6300 EXSTAR. X-ray diffraction experiments were performed at room temperature in a Rigaku Miniflex-II instrument using CuK $\alpha$  radiation ( $\lambda = 1.5406 \text{ \AA}$ ), generated at 30 kV and a current of 15 mA. FTIR Spectrum was taken on Perkin-Elmer Spectrum RX1 Spectrophotometer. The morphology and microstructure of the powders was studied by SEM, with a Nova NanoLab 200 FEG-SEM/FIB, equipped with EDS.

### III. RESULTS AND DISCUSSION

#### 3.1 Thermogravimetric Analysis (TGA-DTG-DTA)

Figure 1 displays TGA-DTG curves of the powdered sample Co:MgAl<sub>2</sub>O<sub>4</sub>. The TG curve, as expected, shows major weight loss at four different temperatures range 35-170°C, 171-270°C, 271-500°C and 501-800°C. Between temperatures 35-170°C (first stage), the weight loss is 12.0% corresponding to loss of free water molecules. Over a temperature range 171-270°C (second stage), the weight loss is nearly 19% and this weight loss could be due to

decomposition of precursors. As compare to MgAl<sub>2</sub>O<sub>4</sub>, weight loss is faster in Co:MgAl<sub>2</sub>O<sub>4</sub>.

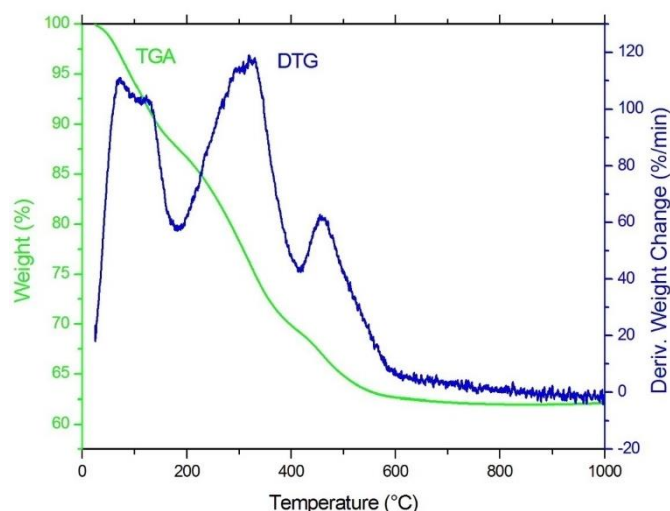


**Figure 1 :** TGA-DTG curves of the Co:MgAl<sub>2</sub>O<sub>4</sub> powder.

The temperatures range 271-500°C (third stage); the rate of weight loss is almost constant (36%), indicating an intermediate structure is formed. Due to decomposition of precursor, a strong peak around temperature 325°C is evident in DTG curve. A shifting in peak position in DTG curve is due to Co<sup>2+</sup> (ionic radii 0.58-0.90 Å). Above 501°C no more detectable weight loss was observed implying no change in phase of the structure. Finally, between temperature 801 and 1000°C TGA-DTG curves exhibit negligible weight loss in the sample, indicating a stable structure of the Co:MgAl<sub>2</sub>O<sub>4</sub>.

Figure 2 shows DTA-TGA results of the dried sample. The DTA curve shows an endothermic reaction below 100°C (typically 30°C and 74°C) which is attributed to the loss of the remaining adsorbed water. At calcination temperature 340°C, endothermic peak suggests formation of Co:MgAl<sub>2</sub>O<sub>4</sub>. A broad exothermic peak is observed in the range 350-500°C this could be attributed to the crystallization of Co:MgAl<sub>2</sub>O<sub>4</sub>. This temperature is significantly lower than that required by the conventional solid-state reaction process where calcination temperature is usually above 1300°C [30]. It is noticed that Co<sup>2+</sup> doped samples crystallize at

relatively higher temperature, i.e. above 850°C as compared to undoped magnesium aluminate that crystallize around 800°C.

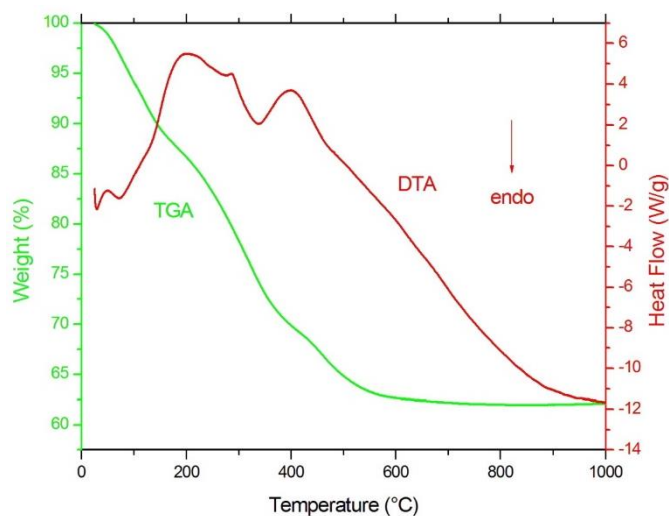


**Figure 2:** TGA-DTA curves of the Co:MgAl<sub>2</sub>O<sub>4</sub> powder.

No exothermic peak on the DTA curve is observed up to temperature 1000°C, indicating that there is no recrystallization of Co:MgAl<sub>2</sub>O<sub>4</sub> spinel. This result shows a good thermal stability of the spinel structure of Co:MgAl<sub>2</sub>O<sub>4</sub> phase at high temperature; a fundamental property for use as catalyst support in reactions at high temperatures. This result is well in agreement with the XRD results as discussed.

### 3.2 X-ray Diffraction (XRD)

Figure 3 depicts the XRD patterns of the samples as-prepared (a) and calcined at temperature 550°C (b), 700°C (c), 850°C (d) and 1000°C (e) for 4h in air. It is observed that the heat treated Co:MgAl<sub>2</sub>O<sub>4</sub> powder shows similar structural evaluation trend as that of MgAl<sub>2</sub>O<sub>4</sub> spinel.

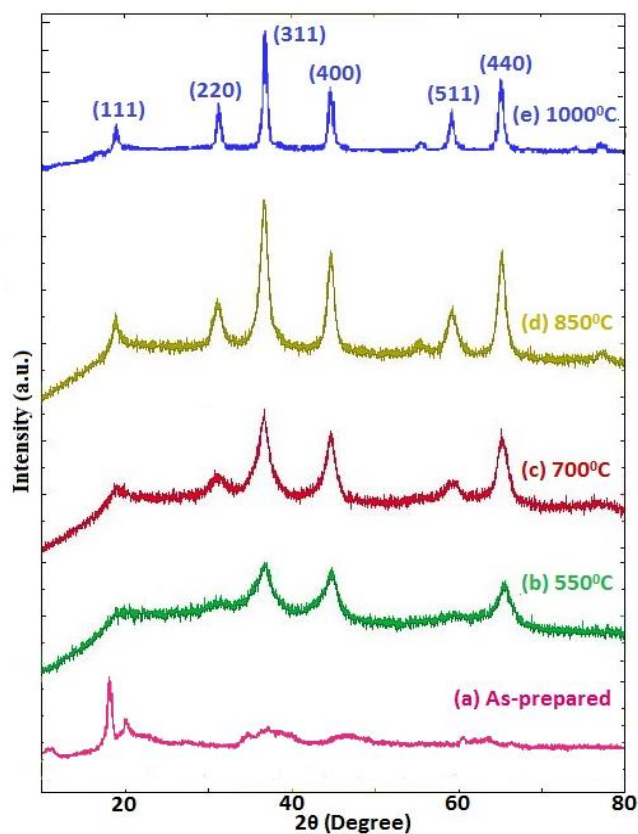


**Figure 3:** XRD patterns of as-prepared and thermally treated samples of Co:MgAl<sub>2</sub>O<sub>4</sub> at different temperatures for 4h.

Diffraction peaks of the sample calcined at 850°C are compared with the standard data of face centred cubic MgAl<sub>2</sub>O<sub>4</sub> [JCPDS 21-1152] and found in accordance with the diffraction peaks of the standard data. The diffraction peaks are indexed by Miller indices (111), (220), (311), (400), (511), (400), respectively with the help of JCPDS data.

Effects of heat treatment on structure parameter of Co:MgAl<sub>2</sub>O<sub>4</sub> like lattice constant, spinel phase, crystallites size and microstrain and dislocation density have also been estimated. Figure 4 displays lattice constant versus Nelson-Riley function.

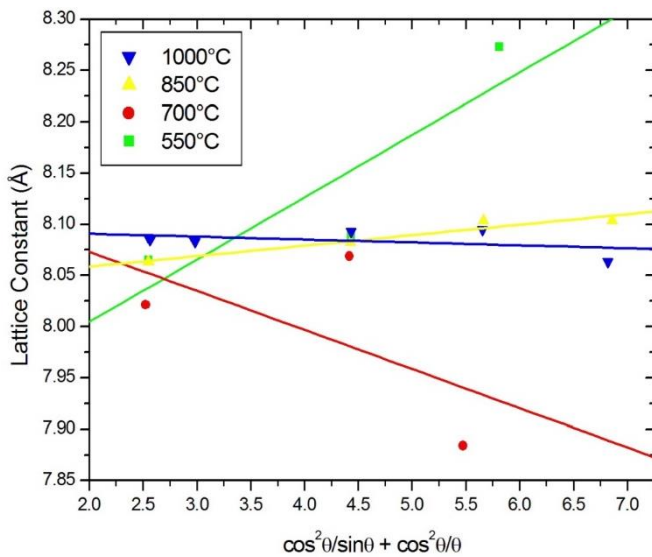


**Figure 4 :** Lattice constant versus Nelson-Riley function

Generally, tendency of divalent and trivalent cations is to occupy tetrahedral and octahedral interstitial sites of spinel but they also enter into the interstitial sites as anti-sites due to many factors, to name a few; ionic radii, electronic configuration and temperature/pressure etc. Let us recall that in  $MgAl_2O_4$ , Al ions (average ionic radius  $\sim 0.45 \text{ \AA}$ ) are smaller than the Mg ions (average ionic radius  $\sim 0.72 \text{ \AA}$ ) and therefore Al ions disperse comparatively faster than the Mg ions. An inequity distribution of cations among interstitial sites are responsible mechanisms for disordering in  $MgAl_2O_4$  spinel nanopowder. The relocation of anti-sites cations between the interstitial sites continues unless its free energy attains a minimum value. Figure 5 illustrates the lattice constant increases with increasing calcination temperature. The increase in lattice constant is due to the fact that the ionic radius of  $Co^{2+}$  ( $0.74 \text{ \AA}$ ) is larger than that of  $Al^{3+}$  ( $0.45 \text{ \AA}$ ) [15] and demonstrates that the  $Co^{2+}$  ions actually enter the crystal lattice and retain the cubic spinel structure [31].

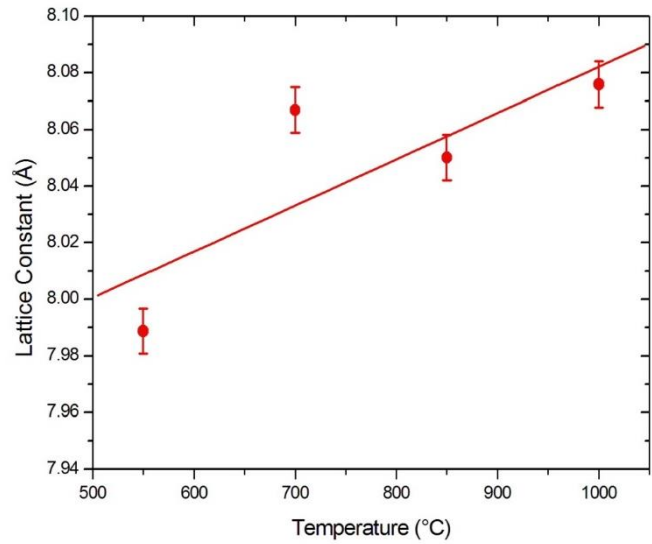


**Figure 5 :** Lattice constant versus calcination temperatures for 4 h.

The effect of temperature on degree of order in  $Co:MgAl_2O_4$  spinel nanopowder is studied and estimated value of degree of order is given in Table 1. The data clearly reveal that the degree of order in  $Co:MgAl_2O_4$  spinel nanopowder increases with increasing calcination temperature (Figure 5).

**Table-1**

Calcined Sample	Crystallite size $D_{D-S}$ (nm)	Crystallite size $D_{W-H}$ (nm)	Strain ( $\epsilon$ )	Lattice constant ( $\text{\AA}$ )	X-ray density ( $\text{g/cm}^3$ )	Dislocation density $\rho = \frac{1}{D_{dis}}$	Degree of ordered phase
550°C(4h)	3.40	2.35	0.0367	7.8831	3.673	0.1815	0.7348
700°C(4h)	5.75	4.36	0.0129	8.1494	3.324	0.0527	0.6957
850°C(4h)	7.78	5.37	0.0121	8.0382	3.464	0.0347	0.8850
1000°C(4h)	15.09	19.33	0.0034	8.0965	3.390	0.0027	0.9901

Crystallite size of  $Co:MgAl_2O_4$  spinel nanopowder is estimated by Debye-Scherrer equation and Williamson-Hall plot (W-H plot) and presented in Table 1. The graph is plotted between  $\sin(\theta_{hkl})$  and  $\beta_{hkl}\cos(\theta_{hkl})$  as shown in Figure 6. The grain size and micro-strain of  $Co:MgAl_2O_4$  do not change significantly in the calcination temperature range  $550^\circ\text{C}$  to  $850^\circ\text{C}$  (4h). In contrast, an increase in crystallite size and a decrease in micro-strain are noticed in a sample heated at  $1000^\circ\text{C}$  (4h). The increase in grain size may be attributed to the fact



that the ionic radius (0.74 Å) and atomic mass of  $\text{Co}^{2+}$  (59 a.m.u.) is larger than that of ionic radius (0.45 Å) and atomic mass (27 a.m.u.) of  $\text{Al}^{3+}$ , respectively.

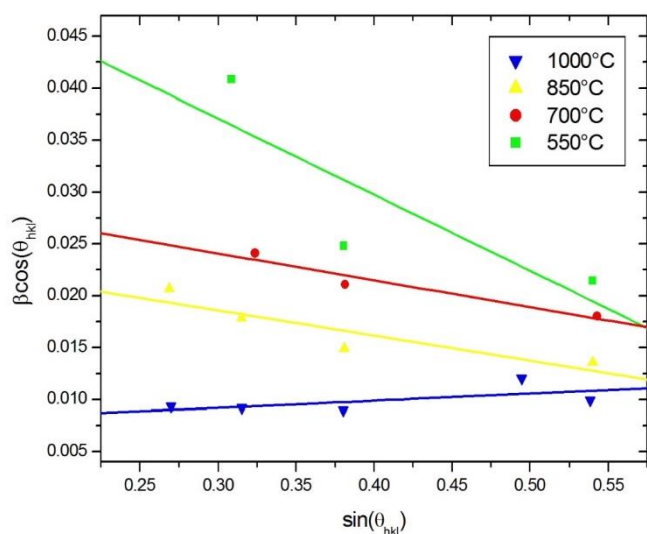


**Figure 6 :** Williamson-Hall plot of calcined of Co:MgAl<sub>2</sub>O<sub>4</sub> spinel nanopowders

The activation energy for the formation of Co:MgAl<sub>2</sub>O<sub>4</sub> is estimated by plotting the graph between crystallite size and calcination temperature (Figure 7).

The plot shows a linear relationship between crystallite size and calcination temperature; and the activation energy is found to be 36 kJ/mol. In case of Co:MgAl<sub>2</sub>O<sub>4</sub> there were two different activation energies (i) for formation of intermediate phase of MgAl<sub>2</sub>O<sub>4</sub> (1.2 kJ/mol) and (ii) for complete formation of MgAl<sub>2</sub>O<sub>4</sub> (53 kJ/mol) because relationship between crystallite size and calcination temperature is nonlinear.

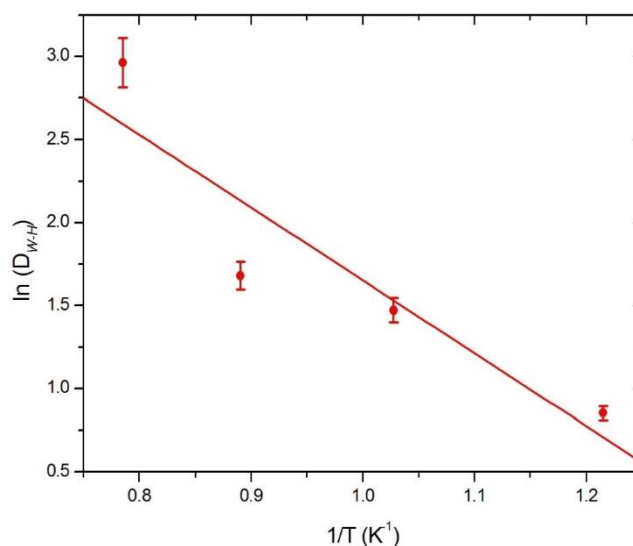


**Figure 7 :** Crystallite size versus calcination temperatures.

Further, by knowledge of average crystallite size and an empirical relation  $\rho \cong \frac{1}{D_{W-H}^2}$ , dislocation density of Co:MgAl<sub>2</sub>O<sub>4</sub> cubic spinel nanocrystallites is obtained and given in Table 1. As calcination temperature is increased, the density of dislocation decreased as a result of less nucleation sites being available during crystallization upon heating, which in turn lead to the comparatively larger crystallite size.

### 3.3 Fourier Transform Infrared (FTIR) Spectroscopy

FTIR Spectroscopy provides valuable information about the phase composition and bonding in the samples. The FTIR of samples as-prepared (a) and calcined at temperature 550°C (b), 700°C (c), 850°C (d) and 1000°C (e) for 4h, in the spectral range of 4000-400  $\text{cm}^{-1}$ , is shown in Figure 8. FTIR spectrum of as-prepared sample (a) shows three distinct strong absorption bands centered around 1357, 1633 and 3523  $\text{cm}^{-1}$ . The absorption band centered around 1357  $\text{cm}^{-1}$  could be ascribed presence of nitrate groups [32]. The bands around 3523  $\text{cm}^{-1}$  and 1633  $\text{cm}^{-1}$  could be assigned as the stretching vibration of H-O-H molecule and the bending modes of H-O-H absorbed

at surface of the product, respectively [33]. The stretching vibration of H-O-H molecules overlaps with surface hydroxyl group vibrations and as a result the stretching band broadens [34]. In FTIR spectroscopy, the bands over range of 1000-400  $\text{cm}^{-1}$  are assigned by metal oxygen bonds (M-O-M) [35]. Narrow band noted around 549  $\text{cm}^{-1}$  may be assigned as mixed hydroxide of magnesium and aluminium [36]. FTIR of Sample (b) shows two distinct signatures : (i) an evaporation of nitrate group which is manifested by elimination of the absorption band centred around 1357  $\text{cm}^{-1}$  and this signature confirms decomposition of nitrates; (ii) broadening in the double hydroxide band.

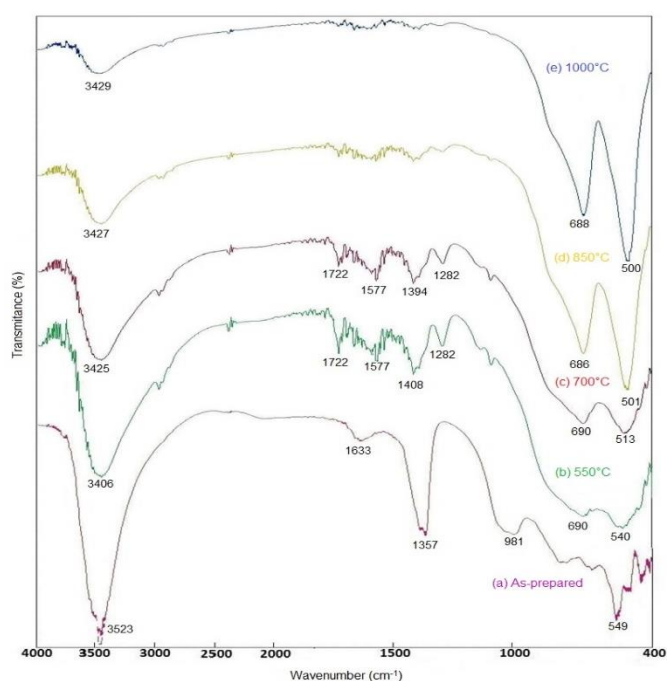


**Figure 8 :** FTIR spectra of as-prepared and thermally treated samples of Cobalt:Magnesium Aluminate at different temperatures for 4h

When calcination temperature was increased up to 700°C and hold for 4h, bands of mixed hydroxides almost disappeared. New weak bands appeared around  $\nu_1=690$  and  $\nu_2=513$   $\text{cm}^{-1}$ , which could be assigned  $\text{AlO}_4$  group [37],  $\text{AlO}_6$  group and  $\text{MgO}$  stretching vibrations, respectively [38, 39]. As the

calcination temperature was increased up to 850°C, the absorption band of  $\text{AlO}_6$  and  $\text{MgO}$  become stronger and evaporation surface water molecules increases as well but absorption band of  $\text{AlO}_4$  diminishes. One may notice that the absorption peak of octahedral site become sharper and stronger in compare to the sample calcined at 700°C. However, thermal treatment at calcination temperature of 1000°C (4h), the appearance of the tetrahedral and octahedral sites band becomes sharp due to the minimization of lattice distortion and enhancement of crystallinity (reduction of surface effect). At calcination temperature 1000°C, the increase in frequency of  $\nu_1$  band occurs due to size effect and the decrease in frequency of  $\nu_2$  arises due to the repulsive dipolar interactions [40]. A significant increase in absorption band at 500  $\text{cm}^{-1}$  (characteristic band of octahedral site) is evident and this could be due to  $\text{Co}^{2+}$  ions actually enter the crystal lattice and retain in the tetrahedral site of cubic spinel structure [31].

The FTIR results are in close agreement with XRD studies. Here, it is worthwhile to point out that even at higher calcination temperature 1000°C for 4h, some OH groups (3429  $\text{cm}^{-1}$ ) remains in the structure. This small amount of water molecules could be due to the inter absorption during the compaction of powder specimen with KBr. The as-prepared powders were light pink, which is attributed to the  $\text{Co}^{2+}$  ions coordinated to six water molecules existing in the coprecipitate. When heated to 700°C, the color of the powders changed to greenish color. At temperature 850°C, the color of the powders changed to blue color which is due to the  $\text{Co}^{2+}$  ions coordinated to four oxygen atom during the formation of  $\text{Co:MgAl}_2\text{O}_4$  nanocrystallites. These results confirm the visual observations (Figure 9) which indicate that the appearance of intense blue color in pigment powder [41].



**Figure 9** : Apparent Color of as-prepared and heat treated  $\text{Co:MgAl}_2\text{O}_4$  samples

### 3.4 Scanning Electron Microscopy (SEM)

The surface morphology of the as-prepared and calcined samples was investigated by SEM equipped with EDS and shown in Figure 10.



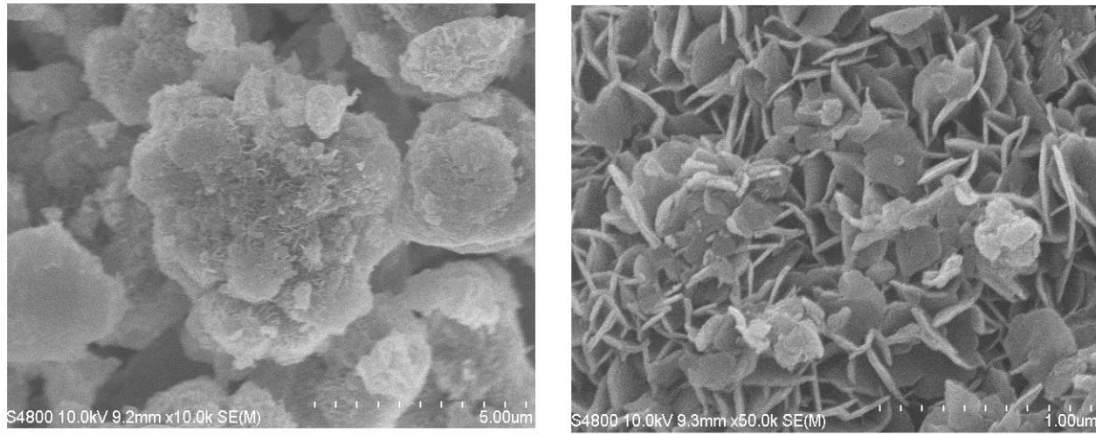


**Figure 10a:** SEM micrographs of as-prepared precursor of Co:MgAl<sub>2</sub>O<sub>4</sub>.

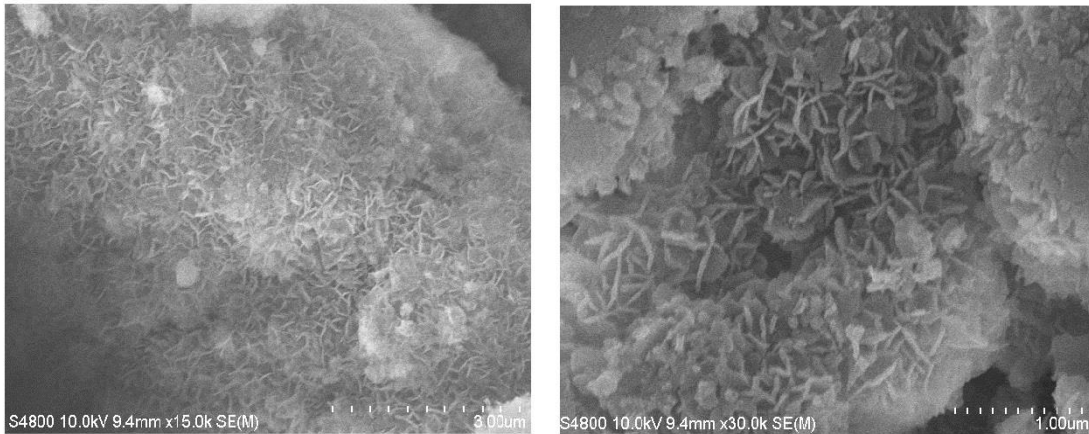


**Figure 10b:** SEM micrographs of Co:MgAl<sub>2</sub>O<sub>4</sub> spinel calcined at 850°C

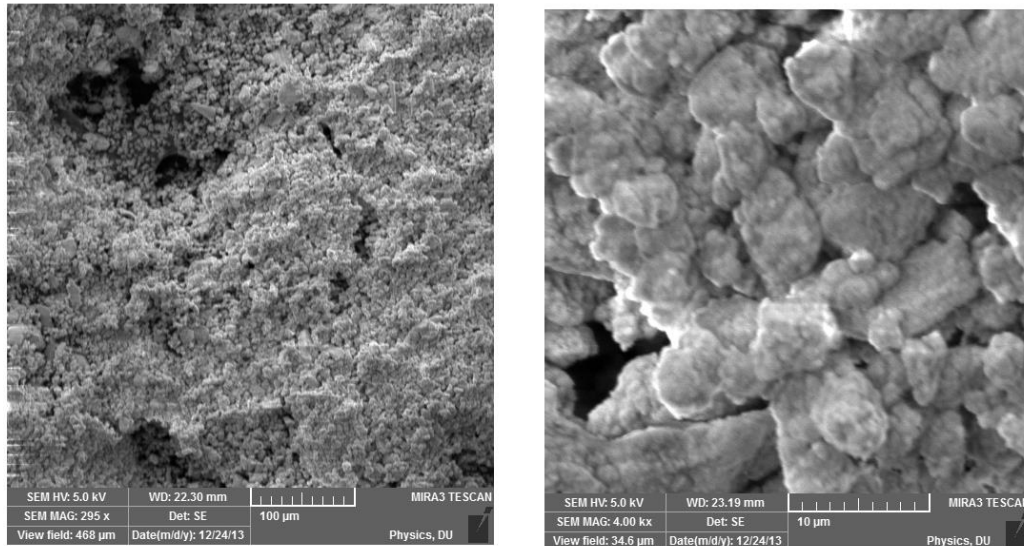


**Figure 10c:** SEM micrographs of Co:MgAl<sub>2</sub>O<sub>4</sub> spinel calcined at 1000°C.

The surface morphology of as-prepared Co:MgAl<sub>2</sub>O<sub>4</sub>, prepared by coprecipitation method, is similar to flower and lamellar structure (Figure 10a), while a structure similar to network is evident when the

sample was calcined at 700°C (Figure 10b). Micrograph shows agglomeration in the powder calcined at 1000°C (Figure 10c). This micrograph

supports increase in size of crystallites of nanoparticles due to coalescence of nanoparticles. Figure 11 illustrates the EDS spectrum of the samples and confirms the presence of cobalt, magnesium, aluminium and oxygen. There is an excess of both Al and O ions relative to Mg ions, in Co:MgAl<sub>2</sub>O<sub>4</sub> ceramic spinel nanopowder. EDS of sample (c) reveals increase cobalt content in the sample and it supports the visual observations of Figure 11.

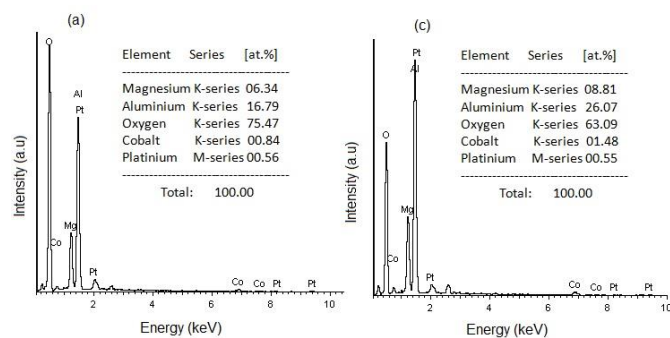


**Figure 11** : EDS of samples as prepared: (a), heat treated at 700°C: (c)

#### IV. SUMMARY

In summary, using precursors: Mg(NO<sub>3</sub>)<sub>2</sub>·6H<sub>2</sub>O, Al(NO<sub>3</sub>)<sub>3</sub>·9H<sub>2</sub>O, Co(NO<sub>3</sub>)<sub>2</sub>·6H<sub>2</sub>O and ammonia solution, as a catalyst, Co:MgAl<sub>2</sub>O<sub>4</sub> cubic spinel nanopowder were prepared by coprecipitation method and subsequently thermal heating was carried out at temperatures 550°C, 700°C, 850°C and 1000°C for 4h, in air. The structural properties of Co:MgAl<sub>2</sub>O<sub>4</sub> nanopowder were investigated by complementary techniques TGA-DTG-DTA, XRD, FTIR and SEM. XRD investigations revealed that at calcination temperature 550°C, an intermediate phase (γ-Al<sub>2</sub>O<sub>3</sub>, a rock salt type structure) of precursor was formed. TGA curve shows that the weight loss is faster in Co:MgAl<sub>2</sub>O<sub>4</sub> compare to the MgAl<sub>2</sub>O<sub>4</sub>. A shifting in peak position is observed in DTG curve, which is due to Co<sup>2+</sup> (ionic radii 0.58-0.90 Å). At calcination temperature 340°C, endothermic peak in DTA curve suggests the formation of Co:MgAl<sub>2</sub>O<sub>4</sub>. Cobalt-magnesium

aluminate crystallizes at relatively higher temperature, i.e. above 850°C as compared to undoped magnesium aluminate that crystallizes around 800°C. An increase in lattice constant is observed, which is due to the fact that the ionic radius of Co<sup>2+</sup> (i.e., 0.745 Å) is larger than that of Al<sup>3+</sup> (0.45 Å). The degree of order in Co:MgAl<sub>2</sub>O<sub>4</sub> spinel nanopowder increases with increasing calcination temperature. The activation energy for the formation of Co:MgAl<sub>2</sub>O<sub>4</sub> is 36 kJ/mol. Nelson-Riely function is a good tool for estimation of lattice parameter for a single phase structure. Results of FTIR and SEM support XRD studies.

Finally, it is concluded that a single phase Co:MgAl<sub>2</sub>O<sub>4</sub> face centred cubic ordered-spinel nanopowder (grain size ~ 20 nm) with a good, chemical homogeneity, is obtained by using coprecipitation method followed by thermal treatment at temperature 1000°C for 4h, in air; and may be used for applications: refractory in heavy industry nano ceramic powders in particular as catalyst support and catalysts by itself, inorganic blue pigments in industry to bring colour to plastics, paints, fibers, papers, rubbers, glass, cement, glazes, ceramics, and porcelain enamels.

#### V. REFERENCES

- [1]. M. B. Camargo, R. D. Stultz, M. Birnbaum and M. Kokta, Co<sup>2+</sup>:YSGG saturable absorber Q switch for infrared erbium lasers, *Opt. Lett.* 20 (1995) 339-341.
- [2]. I. A. Denisov, M. L. Demchuk, N. V. Kuleshov and K. V. Yumashev, Co<sup>2+</sup>:LiGa<sub>5</sub>O<sub>8</sub> saturable absorber passive Q switch for 1.34 μm Nd<sup>3+</sup>:YAlO<sub>3</sub> and 1.54 μm Er<sup>3+</sup>:glass lasers, *Appl. Phys. Lett.* 77 (2000) 2455-2457.
- [3]. N. V. Kuleshov, V. P. Mikhailov, V. G. Scherbitsky, P. V. Prokoshin and K. V. Yumashev, Absorption and luminescence of tetrahedral Co<sup>2+</sup> ion in MgAl<sub>2</sub>O<sub>4</sub>, *J. Lumin.* 55 (1993) 265-269.
- [4]. T. Abritta and F. H. Blak, Luminescence study of ZnGa<sub>2</sub>O<sub>4</sub>: Co<sup>2+</sup>, *J. Lumin.* 48 & 49 (1991) 558-560.

- [5]. K. V. Yumashev, Saturable absorber  $\text{Co}^{2+}:\text{MgAl}_2\text{O}_4$  crystal for Q-switching of 1.34- $\mu\text{m}$   $\text{Nd}^{3+}:\text{YAlO}_3$  and 1.54- $\mu\text{m}$   $\text{Er}^{3+}:\text{glass}$  lasers, *Appl. Opt.* 38 (1999) 6343-6346.
- [6]. J. F. Donegan, F. G. Anderson, F. J. Bergin, T. J. Glynn and G. F. Imbusch, Optical and magnetic-circular-dichroism–optically-detected-magnetic-resonance study of the  $\text{Co}^{2+}$  ion in  $\text{LiGa}_5\text{O}_8$ , *Phys. Rev. B* 45 (1992) 563.
- [7]. I. S. Ahmed, S. A. Shama, M. M. Moustafa, H. A. Dessouki and A. A. Ali, Synthesis and spectral characterization of  $\text{Co}_x\text{Mg}_{1-x}\text{Al}_2\text{O}_4$  as new nano-coloring agent of ceramic pigment, *Spectrochimica Acta A* 74 (2009) 665-672.
- [8]. A. E. Giannakas, A. K. Ladavos, G. S. Armatas and P. J. Pomonis, Surface properties, extural features and catalytic performance for  $\text{NO} + \text{CO}$  abatement of spinels  $\text{MAl}_2\text{O}_4$  ( $\text{M} = \text{Mg}, \text{Co}$  and  $\text{Zn}$ ) developed by reverse and bicontinuous microemulsion method, *Appl. Surface Sc.* 253 (2007) 6969-6979.
- [9]. M. Llusar, A. Forés, J. A. Badenes, J. Calbo, M. A. Tena and G. Monrós, Colour analysis of some cobalt-based blue pigments, *J. of Eur. Ceram. Soc.*, 21 (2001) 1121-1130.
- [10]. W. Li, J. Li and J. Guo, Synthesis and characterization of nanocrystalline  $\text{CoAl}_2\text{O}_4$  spinel powder by low temperature combustion, *J. of Eur. Ceram. Soc.* 23(2003) 2289-2295
- [11]. C. Luan, D. Yuan, X. Duan, H. Sun, G. Zhang, S. Guo, Z. Sun, D. Pan, X. Shi and Z. Li, Synthesis and characterization of  $\text{Co}^{2+}:\text{MgAl}_2\text{O}_4$  nanocrystal, *J. Sol-Gel Sci. Techn.* 38 (2006) 245-249.
- [12]. X. L. Duan, C. F. Song, Y.C. Wu, F. P. Yu, X. F. Cheng and D. R. Yuan, Preparation and optical properties of nanoscale  $\text{MgAl}_2\text{O}_4$  powders doped with  $\text{Co}^{2+}$  ions, *J. of Non-Cryst. Solids* 354 (2008) 3516-3519.
- [13]. M. J. Iqbal and B. Kishwar, Electrical properties of  $\text{MgAl}_2-2x\text{ZrxMxO}_4$  ( $\text{M} = \text{Co}, \text{Ni}$  and  $x = 0.00-0.20$ ) synthesized by coprecipitation technique using urea, *Mater. Res. Bull.* 44 (2009) 753-758.
- [14]. M. J. Iqbal, B. Ismail, C. Rentenberger and H. Ipser, Modification of the physical properties of semiconducting  $\text{MgAl}_2\text{O}_4$  by doping with a binary mixture of  $\text{Co}$  and  $\text{Zn}$  ions, *Mater. Res. Bull.* 46 (2011) 2271-2277.
- [15]. J. Ahmad, M. Q. Awan, M. E. Mazhar and M. N. Ashiq, Effect of substitution of  $\text{Co}^{2+}$  ions on the structural and electrical properties of nanosized magnesium aluminate, *Physica B* 406 (2011) 254-258.
- [16]. L. Torkian, M. Daghighi and Z. Boorboor, Simple and Efficient Rout for Synthesis of Spinel Nanopigments, *J. of Chemistry* (2013), Article ID 694531, DOI: 10.1155/2013/694531
- [17]. B. Thomas and M. A. Khadar, Dielectric properties of nano-particles of zinc sulphide, *Pramana J. Phys.* 45 (1995) 431-438.
- [18]. G. A. Slack, F. S. Ham and R. M. Chrenko, Optical Absorption of Tetrahedral  $\text{Fe}^{2+}$  ( $3d^6$ ) in Cubic  $\text{ZnS}$ ,  $\text{CdTe}$ , and  $\text{MgAl}_2\text{O}_4$ , *Phys. Rev.* 152 (1966) 376.
- [19]. E. S. Gaffney, Spectra of Tetrahedral  $\text{Fe}^{2+}$  in  $\text{MgAl}_2\text{O}_4$ , *Phys. Rev. B* 8 (1973) 3484.
- [20]. A. D. Giusta, S. Carbonin and G. Ottonello, Temperature-dependent disorder in  $\text{Mg-Al-Fe}^{2+}\text{-Fe}^{3+}$ -spinel a natural, *Miner. Mag.* 60 (1996) 603-616.
- [21]. T. N. Michail, M. K. Muller and K. Langer, Electronic absorption spectroscopy of natural ( $\text{Fe}^{2+}$ ,  $\text{Fe}^{3+}$ )-bearing spinels of spinel s.s.-hercynite and gahnite-hercynite solid solutions at different temperatures and high-pressures, *Phys. Chem. Miner.* 32 (2005) 175-188.
- [22]. W. Ying, K.X. Yu, Y. Xiong and W. Hui, EPR investigation of the site symmetry of  $\text{Fe}^{3+}$  ions in the spinel crystals, *Physica B* 381 (2006) 260-264.
- [23]. S. Britto, A. V. Radha, N. Ravishankar and P. V. Kamath, Solution decomposition of the layered double hydroxide (LDH) of  $\text{Zn}$  with  $\text{Al}$ , *Solid State Sciences* 9 (2007) 279-286.
- [24]. T. Suzuki, H. Nagai and M. Nohara, Melting of antiferromagnetic ordering in spinel oxide  $\text{CoAl}_2\text{O}_4$ , *Journal of Physics*, 19 (2007), Article ID145265.
- [25]. Z. Chen, E. Shi and Y. Zheng, Hydrothermal synthesis of nanosized  $\text{CoAl}_2\text{O}_4$  on  $\text{ZnAl}_2\text{O}_4$  seed crystallites, *J. of Am. Ceram. Soc.* 86 (2003) 1058-1060.

- [26]. A. T. Aruna and A. S. Mukasyan, Combustion synthesis and nanomaterials, *Current Opinion in Solid State & Mater. Sc.* 12 (2008) 44-50.
- [27]. R. Ianos and R. Laza, Combustion synthesis, characterization and sintering behavior of magnesium aluminate (MgAl<sub>2</sub>O<sub>4</sub>) powders, *Mater. Chem. and Phys.*, 115 (2009) 645-648.
- [28]. K. V. Yumashev, N. N. Posnov and V. P. Mikhailov, Excited-state absorption and stimulated emission of tetrahedral Co<sup>2+</sup> ion in LiGa<sub>5</sub>O<sub>8</sub>, *Appl Phys B* 69 (1999) 41-44.
- [29]. K. V. Yumashev, I. A. Denisov, N. N. Posnov, P. V. Prokoshin and V. P. Mikhailov, Nonlinear absorption properties of Co<sup>2+</sup>:MgAl<sub>2</sub>O<sub>4</sub> crystal, *Appl. Phys. B* 70 (2000) 179-184.
- [30]. H. V. Keer, M. G. Bodas, A. Bhaduri and A. B. Biswas, Studies on Mn<sub>3</sub>O<sub>4</sub> & MgAl<sub>2</sub>O<sub>4</sub> system, *J. Inorg. Nucl. Chem.* 37 (1975) 1605-1607.
- [31]. M. J. Iqbal and S. Farooq, Effect of doping of divalent and trivalent metal ions on the structural and electrical properties of magnesium aluminate, *Mater. Sci. Eng. B* 136 (2007) 140-147.
- [32]. K. Vivekanandan, S. Selvasekarapandian and P. Kolandaivel, Raman and FTIR studies of Pb<sub>4</sub>(NO<sub>3</sub>)<sub>2</sub>(PO<sub>4</sub>)<sub>2</sub>·2H<sub>2</sub>O crystal, *Mater. Chem. Phys.* 39 (1995) 284-289.
- [33]. M. A. Ulibarri, C. Barriga and J. Cornejo, Kinetics of the thermal dehydration of some layered hydroxycarbonates, *Thermochim. Acta* 135 (1988) 231-236.
- [34]. P. Aghamkar, S. Duhan, M. Singh, N. Kishore and P. K. Sen, Effect of thermal annealing on Nd<sub>2</sub>O<sub>3</sub>-doped silica powder prepared by the solgel process, *J. Sol-Gel Sci. Technol.* 46 (2008) 17-22.
- [35]. J. Parmentier, M. Richard-Plouet and S. Vilminot, Influence of the sol-gel synthesis on the formation of spinel MgAl<sub>2</sub>O<sub>4</sub>, *Mater. Res. Bull.* 33 (1998) 1717-1724.
- [36]. R. V. Prikhod'ko, M. V. Sychev, I. M. Astrelin, K. Erdmann, A. Mangel and R. A. Van Santen, Synthesis and Structural Transformations of Hydrotalcite-like Materials Mg<sub>3</sub>Al and Zn<sub>3</sub>Al, *Russ. J. Appl. Chem.* 74 (2001) 1621-1626.
- [37]. F. Meyer, R. Hempelmann, S. Mathur and M. Veith, Microemulsion mediated sol-gel synthesis of nano scaled MAI<sub>2</sub>O<sub>4</sub> (M= Co, Ni, Cu) spinels from single-Source Heterobimetallic Alkoxide precursor, *J. Mater. Chem.* 9 (1999) 1755-1763.
- [38]. F. T. Li, Y. Zhaoa, L. Ying, H. J. Ying, L. R. Hong and D. Zhaob, Solution combustion synthesis and visible light-induced photocatalytic activity of mixed amorphous and crystalline MgAl<sub>2</sub>O<sub>4</sub> nanopowders, *Chem. Eng. J.* 173 (2011) 750-759.
- [39]. A. I. Gusev and A. A. Rempel, *Nanocrystalline Materials*, Cambridge International Science Publication Cambridge, (2004).
- [40]. Jr E. H. Walker, J. W. Owens, M. Etienne and D. Walker, The novel low temperature synthesis of nanocrystalline MgAl<sub>2</sub>O<sub>4</sub> spinel using "gel" precursors, *Mater. Res. Bull.* 37 (2002) 1041-1050.
- [41]. L. K. C. de Souza, J. R. Zamian, G. N. da Rocha Filho, Luiz E.B. Soledadeb, Ieda M.G. dos Santosb, Antonio G. Souzaab, Thomas Schellerc, Rômulo S. Angélicac and Carlos E. F. da Costaa, Blue pigments based on CoxZn<sub>1-x</sub>Al<sub>2</sub>O<sub>4</sub> spinels synthesized by the polymeric precursor method, *Dyes and Pigments*, 81 (2009) 187-192.

#### Cite this Article

Dr. Shyam Sunder, Dr. Wazir Singh, "Thermal Evolution and Structural Study of Cobalt Doped Magnesium Aluminate Spinel Nanoparticles Prepared by Coprecipitation Technique", *International Journal of Scientific Research in Science, Engineering and Technology (IJSRSET)*, Online ISSN : 2394-4099, Print ISSN : 2395-1990, Volume 4 Issue 7, pp. 712-723, March-April 2018.

Journal URL : <http://ijsrset.com/IJSRSET18441154>